CRYSTAL GROWTH & DESIGN

pubs.acs.org/crystal

Article

Quantum Chemical Modeling of Mechanical Properties of Aspirin Polymorphic Modifications

Yevhenii Vaksler, Abdenacer Idrissi, Victoriya V. Urzhuntseva, and Svitlana V. Shishkina*

Cite This: *Cryst. Growth Des.* 2021, 21, 2176–2186

Read Online

ACCESS | Metrics & More | Article Recommendations | Supporting Information

ABSTRACT: Being well studied, **I** and **II** polymorphic structures of aspirin are very suitable for testing a new method to study mechanical properties using quantum chemical calculations. The proposed method consists of two steps: analysis of the pairwise interaction energies between molecules in a structure obtained by the X-ray diffraction study with separation of strongly bound fragments and further quantum chemical modeling of their displacement in relation to each other. Application of this method to aspirin polymorphs **I** and **II** showed that they have layered structure and the [001] crystallographic direction within the (100) plane is the most probable for a shear deformation, which correlates well with the data of the nanoindentation method. The energy barriers for the displacement in this direction were calculated as 17.1 and 14.5 kcal/mol for polymorphs **I** and **II**, respectively. It was shown that the area of strong repulsion between molecules belonging to the neighboring layers can complicate shear deformation in stable crystal forms **I** and **II** of aspirin. A similar study of the latest polymorph **IV** showed that this structure is not layered but columnar. The easiest shear deformations are possible for the displacement in the [010] crystallographic direction within the (100), (−101), and (001) planes. The low-energy barriers for these displacements (5.4, 8.8, and 9.5 kcal/mol, respectively) and the absence of significant repulsion along all the translation may explain the metastability of this structure. The proposed method is a good tool to predict mechanical properties.

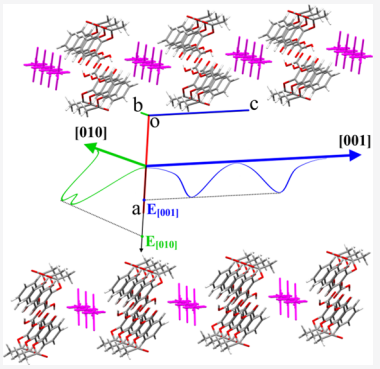

INTRODUCTION

A large number of drugs and other functional materials are used in the crystalline state because of their higher chemical stability in the solid phase compared with the solution.[1] However, the crystalline state turned out to have some features caused by the molecule ability to form various conformations and/or sets of intermolecular interactions. This phenomenon is known as polymorphism.[2] Polymorphism proved to be the most important phenomenon for the pharmaceutical industry due to the fact that different crystal forms of one compound have different properties directly related to their manufacturability (compactability, hardness, tabletting, tensile strength, etc.) and bioavailability (solubility and dissolution rate).[3] Therefore, choice of the most efficient crystal form of API is the key stage of a drug development.

Unfortunately, a crystal form may happen to be unstable and transforms into a new phase depending on handling, manufacturing, processing, or storage. Therefore, polymorphic transitions of well-known drugs are of special interest for both fundamental and practical reasons.[4−10] The most crucial result of such a transformation is the change of solubility and dissolution rate influencing the biological properties of a drug as it happened with the antiretroviral drug ritonavir (the trade mark is Norvir).[11] So, control of the crystalline state is necessary at all key stages of manufacturing and storage of a solid form.

Possible changes of a crystal structure under external mechanical influence are known as mechanical properties and may be caused by peculiarities of a crystal packing. Mechanical properties of molecular crystals are studied by both experimental and theoretical methods. The nanoindentation method[12] and the diamond anvil cell technique[13,14] are the most used experimental methods. Each of them has its own merits and shortcomings, but both experimental methods require special expensive equipment. Application of quantum chemistry methods may help to tackle this problem.[15] Periodic calculations of a crystal structure allow us to estimate the attachment energy for the prediction of the most probable slip plane[16] or to calculate the elastic constants associated with mechanical deformations.[17,18] However, such calculations depend crucially on initial parameters and require substantial computational resource.

Obviously, mechanical properties of molecular crystals are associated with anisotropy of a crystal structure. Therefore, a reliable method of crystal structure analysis is of great

Received: November 28, 2020
Revised: February 18, 2021
Published: February 25, 2021

https://dx.doi.org/10.1021/acs.cgd.0c01613
Cryst. Growth Des. 2021, 21, 2176–2186

importance. The recently proposed method based on pairwise interaction energies between molecules studying makes it possible to separate out strongly bound motifs of a crystal packing using simple and inexpensive quantum chemical calculations.[19−21] It is known that weak interactions between separated structural motifs are crucial for mechanical response of a crystal.[22−26] Therefore, such an analysis opens a way to determine possible directions of the easiest deformation of a crystal structure. Some attempts to model a crystal deformation using quantum chemical calculations at the AM1 semiempirical level[27] or within periodic boundary[28] have been performed recently. However, the proposed approaches require further development and improvement.

Polymorphic modifications of aspirin were chosen as very suitable for the development of a more systematic method of mechanical properties of molecular crystal modeling using quantum chemical calculations. Aspirin is a well-studied drug, so the results obtained within a new approach can be compared with the available experimental and theoretical data. For a very long time, the existence of aspirin polymorphs remained questionable.[29−34] The crystal structure of the polymorph **II** was obtained only in 2005 by Zaworotko and co-workers.[35] However, a very subtle difference between polymorphs **I** and **II** as well as low quality of the experimental data required additional evidence. Further studies of the new crystal form of aspirin showed that it was not a twin or a mixture of form **I** and form **II** but an intergrown crystal containing domains of both forms **I** and **II**.[36,37] The pure polymorphic form **II** was crystallized only in 2011.[38] Polymorphic modifications were thoroughly studied by experimental[39−43] and theoretical methods.[44−47] Particular attention was paid to the study of possible polymorphic transitions of aspirin polymorphs.[42] The transition of the less stable form **II** into form **I** was proven under grinding.[41] The preview of polymorph **III** obtained at the pressure above ∼2 GPa from the polymorph **I** was based on Raman spectroscopy data.[42] Unfortunately, the structure of this polymorph was not proven reliably. The study of mechanical properties of polymorphic structures **I** and **II** led to clear definition of the (100) crystallographic plane along which shear deformation is the easiest.[41,42,47,48] However, the crystallographic directions for the easiest deformation within this plane were not determined unambiguously.[41,42,48] The newest ambient polymorph of aspirin (form **IV** according to the original publication[49]) was solved from the powder diffraction data only in 2017 and turned out to be metastable, so its mechanical properties are still not studied.

In the present study, a new method to model mechanical properties is proposed and verified using known experimental and theoretical data for forms **I** and **II** of aspirin. In addition, possible mechanical response of metastable polymorphic form **IV** is predicted.

EXPERIMENTAL SECTION

Analysis of Crystal Structures from the Energetic Viewpoint. The three aspirin polymorphic structures with refcodes ACSALA14,[36] ACSALA15,[37] ACSALA23[49] (Figure S1) have been extracted from the Cambridge Crystal Structure Database.[50] Crystal structure analysis was performed within the approach based on quantum chemical calculations of pairwise interaction energies between molecules in a crystal.[51,52] Any molecule in a crystal may be considered as basic, and its first coordination sphere can be constructed using the standard procedure within the Mercury program.[53] This option allows us to determine all molecules for which the distance between atoms of the basic molecule and its symmetric equivalent is shorter than van der Waals radii sum plus 1 Å at least for one pair of atoms. In the case of $Z' > 1$, this procedure should be applied to each of the molecules in the asymmetric part of the unit cell. The selected fragment of the crystal packing was divided into dimers where one molecule is basic and the other one belongs to its first coordination sphere. The molecular geometries of these dimers were not optimized. Taking into account the well-known effect of X−H bonds shortening in the X-ray diffraction study,[54] the positions of hydrogen atoms were normalized to 1.089 Å for C−H and 0.993 Å for O−H bonds, according to neutron diffraction data.[55] The pairwise interaction energies were calculated using the B97D3 density functional method[56] with def2-TZVP basis set[57,58] and corrected for basis set superposition error by the counterpoise method.[59] The choice of the calculation method is based on the benchmark study of accurate estimation of pairwise interaction energies.[60] All single-point calculations were performed within the Gaussian03 software.[61]

The energy-vector diagrams (EVD) were used for the graphic representation of the obtained data. The calculated interaction energy between two molecules in a crystal may be described by a vector directed from the geometrical center of one molecule toward the geometrical center of the second molecules.[52] This approach to the set of the pairwise interaction energies between a basic molecule (0) and each of the molecules belonging to its first coordination sphere (i) makes it possible to visualize the calculated energies as a set of such vectors (L_i) coming from the geometrical center of a basic molecule. The length of each energy vector L_i is calculated using the following equation

$$L_i = \frac{R_i E_i}{2E_{str}} \quad (1)$$

where R_i is the distance between the geometric centers of the interacting molecules, E_i is the interaction energy between these two molecules, and E_{str} is the energy of the strongest pairwise interaction in the crystal.

The basic molecule may be replaced by its vector image, and all symmetry operations can be applied to this image. As a result, the crystal structure can be analyzed in terms of interaction energies between molecules or strongly bound structural motifs of a crystal packing. The building unit (BU), primary basic structural motif (BSM_1) and secondary basic structural motif (BSM_2) can be separated out, and interaction energies within these strongly bound fragments and between them can be analyzed. Full list of interaction energies, symmetry codes and bonding types of the monomeric and dimeric BUs in polymorphs **I**, **II**, and **IV** is presented in Tables S1−S6.

Modeling of a Shear Deformation. The results of the crystal structure analysis based on the pairwise interaction energies study were used to model possible mechanical response of a crystal packing. In reality, all interactions between molecules can be deformed under external stress but the weakest interactions are expected to be the most deformed. Therefore, it was presumed as a model approximation that the shear deformation is possible along the weakest plane between strongly bound fragments and it is not accompanied by the deformation of these fragments themselves.

The fragment of the secondary structural motif (BSM_2) used as a fixed part in the modeling and one BU belonging to the neighboring BSM_2 used as a mobile part were extracted from the crystal structure as a rigid unit and used as a model system. For the shear simulation, the mobile part of the chosen system was shifted along the fixed part on one crystallographic translation with a certain step size. The single-point interaction energies between mobile and fixed fragments were calculated for each point along the translation trajectory using B97D3 functional and cc-PVDZ basis set[62,63] within the Gaussian03 software and corrected for basis set superposition error by the counterpoise method.[59] The shift energy profile was constructed as a function of calculated interaction energy and the shift of a mobile part in relation to the initial position. The shift energy barrier was calculated as a

https://dx.doi.org/10.1021/acs.cgd.0c01613
Cryst. Growth Des. 2021, 21, 2176−2186

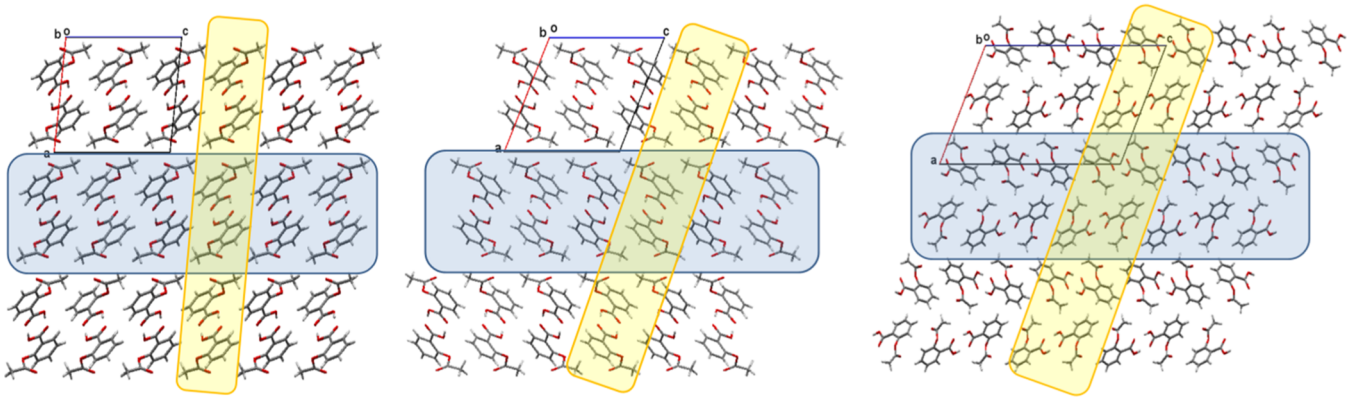

Figure 1. Crystal structure of polymorphic forms **I** (on the left), **II** (in the middle), and **IV** (on the right) of aspirin. Layers of centrosymmetric dimers parallel to the (100) crystallographic plane are highlighted in blue; layers of centrosymmetric dimers parallel to the (001) crystallographic plane are highlighted in yellow.

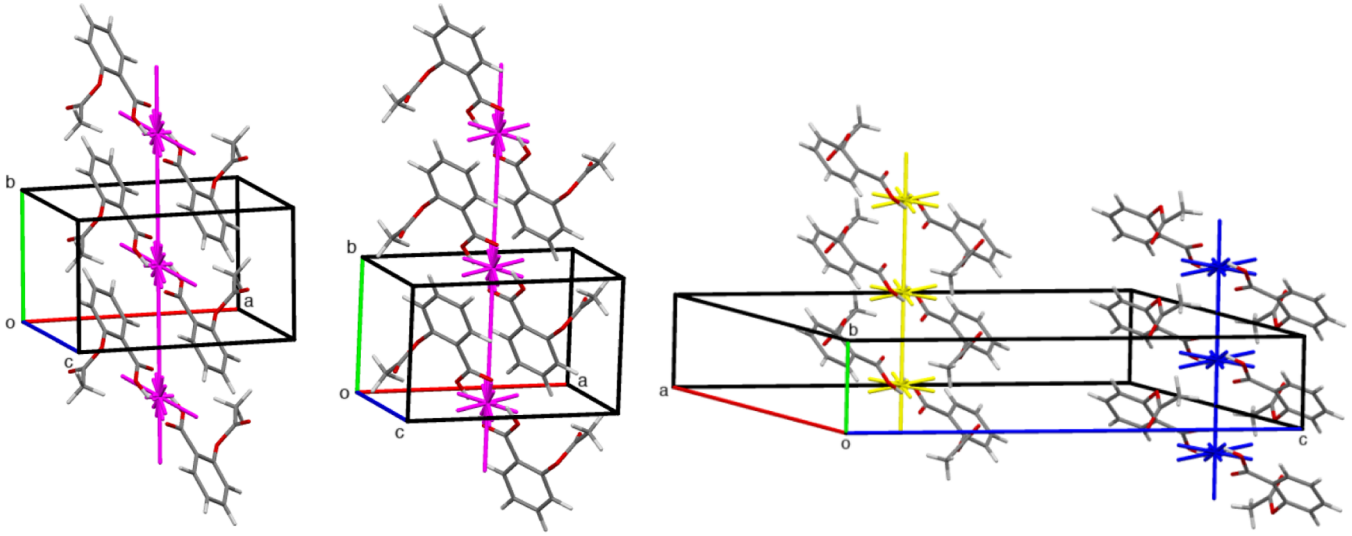

Figure 2. Columns in the [010] crystallographic direction as the primary basic structural motif in terms of molecules and EVDs in polymorphic structures **I** (on the left), **II** (in the middle), and **IV** (on the right). EVD for columns of A and B types are highlighted in yellow and blue, respectively, in structure **IV**.

difference between the highest and lowest interaction energies between the mobile and fixed parts within the translation.

RESULTS AND DISCUSSION

The crystal structures of aspirin polymorphs **I** and **II** have been thoroughly studied.[36,37] However, only hydrogen bonds of various types and their geometric characteristics were discussed and layers of centrosymmetric dimers as a structural motif of the crystal packing were highlighted. Such an analysis did not take into account non-directed interactions between molecules like electrostatic, general dispersion, polarization, and so forth. Also, stacking between π-systems was not mentioned due to the impossibility of unambiguous description of this interaction. The crystal structure of polymorphic form **IV** proved to be more complicated due to the presence of two molecules in the unit cell asymmetric part. This structure was also characterized as layered.[49]

Two types of layers may be visualized in all the studied structures of aspirin (Figure 1). There are no specific intermolecular interactions between molecules belonging to the neighboring layers. Therefore, the choice of the plane in which the easiest way of crystal packing deformation may occur can be made on the basis of the interaction energies between strongly bound structural motifs. To evaluate these energies, the analysis of a crystal packing based on the study of pairwise interaction energies between molecules should be applied.

Crystal Packing Analysis Based on the Study of Pairwise Interaction Energies. At the first stage of the analysis, the molecule was considered a BU and its first coordination sphere was constructed. In the case of polymorphic form **IV**, the first coordination sphere was constructed separately for each of the molecules A and B found in the asymmetric part of the unit cell. The basic molecule is surrounded by 14 neighbors in polymorphic form **I** and only by 13 in polymorphs **II** and **IV** (Tables S1−S3 in Supporting Information). At that, the total interaction energy of the basic molecule with all the molecules belonging to its first coordination sphere is −63.2 kcal/mol in polymorphic structure **I**, −64.3 kcal/mol in structure **II**, and −62.2 kcal/mol (the basic molecule A) or −59.3 kcal/mol (the basic molecule B) in structure **IV**. The basic molecule forms the strongest interaction with only one neighboring molecule due to O−H···O hydrogen bonds in all the aspirin polymorphs. The

https://dx.doi.org/10.1021/acs.cgd.0c01613
Cryst. Growth Des. 2021, 21, 2176−2186

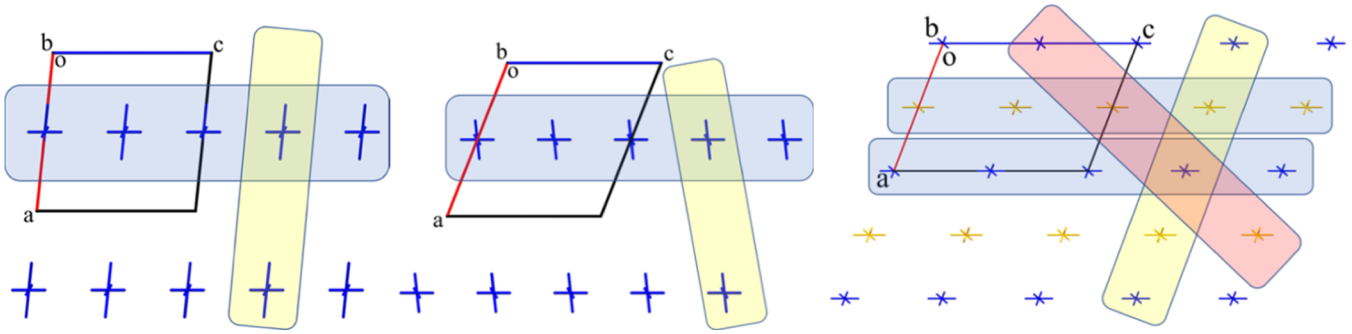

Figure 3. Packing of columns in terms of EVDs, projection along the [010] crystallographic direction for polymorphic structures **I** (on the left), **II** (in the middle), and **IV** (on the right). Possible layers are highlighted in different colors: layers parallel to the (100) crystallographic plane are blue; layers parallel to the (001) plane in structures **I** and **IV** or to the (−102) plane in structure **II** are yellow; and a layer parallel to the (−101) plane in structure **IV** is red.

Table 1. Interaction Energies (in kcal/mol) between Dimeric BUs within Separated Structural Motifs and between Them

structural motif	I		II			IVAA		IVBB		
BSM_1	−26.8		−26.9			−35.3		−32.9		
	(100)	(001)	(100)	(−102)	(100)	(001)	(−101)	(100)	(001)	(−101)
BSM_1/BSM_1	**−16.6**	−6.5	**−16.8**	−6.7	**−9.9**	**−8.7**	−3.6	**−10.5**	**−8.7**	−3.6
BSM_2	**−59.9**	−39.0	**−60.5**	−40.1	**−55.0**	**−52.8**	−42.5	**−53.8**	**−50.3**	−40.1
BSM_2/BSM_2	−7.7	−18.2	−7.4	−17.6	**−12.3**	**−13.5**	−18.6	**−12.3**	**−14.1**	−19.2

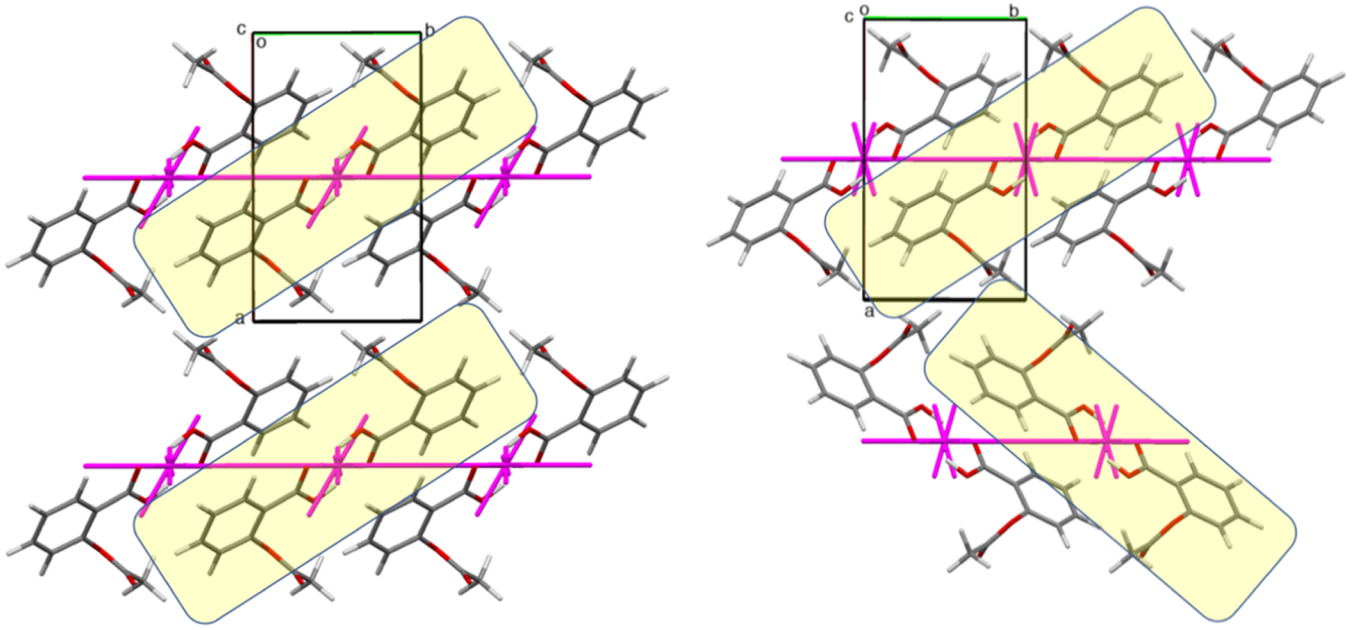

Figure 4. Relative positions of centrosymmetric dimers belonging to the neighboring columns within the (001) crystallographic plane in structure **I** (on the left) and the (−102) crystallographic plane in structure **II** (on the right). Dimeric BUs are highlighted in yellow.

interaction energy between the molecules in this centrosymmetric dimer is more than three times higher than the interaction energies of the basic molecule with other neighboring ones (Figure S2). Therefore, the BU of the aspirin polymorphic structures is not a molecule but a centrosymmetric dimer.[18] It should also be noted that dimers of AA or BB types are the BUs in the polymorphic structure **IV**.

These dimeric BUs were used for further analysis to separate out some structural motifs of a crystal packing and evaluate the interaction energies between them. For this purpose, the first coordination sphere of the dimeric BU contains 18 neighboring dimers in polymorphic structure **I** and 16 neighboring ones in structure **II**. At that, the total energy of BU interaction with all the surrounding dimers is equal (−75.3 kcal/mol) in these polymorphic structures (Tables S4−S6 in Supporting Information). Each of the AA and BB dimers is surrounded by 16 neighboring dimers of different types, but the total interaction energies of the BU with its first coordination sphere are slightly different (−79.7 kcal/mol for BU AA and −78.5 kcal/mol for BU BB).

Each BU forms two strongest interactions with equal energies (Tables S4−S6, Figure S3) between dimers that are located in opposite directions along the [010] crystallographic

https://dx.doi.org/10.1021/acs.cgd.0c01613
Cryst. Growth Des. 2021, 21, 2176−2186

axis. As a result, the linear column in the direction [010] can be separated out as the primary basic structural motif (BSM1) in all the three polymorphs of aspirin (Figure 2). Moreover, the columns containing only dimers AA (the EVD is colored yellow) and the columns of dimers BB (EVD is colored blue) are observed in structure **IV**. Stacking and nonspecific interactions are found between dimeric BUs within these columns. The total interaction energy of the BU within the column is −26.8 kcal/mol in polymorph **I**, −26.9 kcal/mol in polymorph **II**, and −35.3 kcal/mol (column A) or −32.9 kcal/mol (column B) in polymorph **IV**.

Further analysis of the interaction energies between dimeric BUs belonging to neighboring columns makes it possible to discuss the formation of layers as the second basic structural motifs in the crystals **I**, **II**, and **IV** (Figure 3). Each column is surrounded by eight neighboring ones in all the studied crystals. The basic column interacts strongly with two columns lying in opposite directions within the (100) crystallographic plane in crystals **I** and **II**. As a result, the layers parallel to the (100) crystallographic plane may be regarded as a secondary basic structural motif (BSM_2) in structures **I** and **II**. The C−H···π and non-specific interactions are found between molecules of the neighboring columns within the layer. Within the BSM_2, the total interaction energies between the dimeric BU and the neighboring dimeric ones are almost 8 times higher than the interaction energies between those belonging to the layers parallel to the (100) crystallographic plane (Table 1). It should be noted that the structure of the BSM_1 and BSM_2 [layer parallel to the (100) plane] is the same as in polymorphs **I** and **II** of aspirin. The main difference between these crystals can be caused by the relative position of the neighboring layers.

According to the calculated pairwise interaction energies, the dimeric BU interacts strongly with two neighboring ones lying in opposite directions within the (001) crystallographic plane in structure **I** or the (−102) plane in structure **II** (Figure 3, layers are highlighted in yellow) which may be considered as an alternative BSM_2. The interaction energies between BSM_1 within these planes are smaller as compared to those within the (100) planes mentioned above (Table 1). It may be caused by the extremely weak C−H···O intermolecular interactions between molecules of the neighboring columns lying in the (001) plane in structure **I** or the (−102) plane in structure **II**. Moreover, relative orientation of centrosymmetric dimers belonging to the neighboring columns within these planes is different (Figure 4). Total interaction energies of the dimeric BU with the neighboring ones within the (001) (structure **I**) or (−102) (structure **II**) crystallographic planes as BSM_2 are twice as strong as those between them (Table 1).

Comparison of the energy ratio inside and between BSM_1 and BSM_2 (Table 1) makes it possible to come to the conclusion that the polymorphic crystals of aspirin **I** and **II** have the columnar-layered structure, where layers parallel to the (100) crystallographic plane are the most strongly bound secondary basic structural motifs (BSM_2). The main difference between these polymorphic forms of aspirin is the relative orientation of the dimeric BUs belonging to neighboring layers (Figure 4). Such a conclusion would not have been possible without the analysis of the energetic structure and strongly bound structural motifs in these crystals.

As it was mentioned above, the analysis of polymorphic structure **IV** is more complicated due to the presence of two molecules in the asymmetric part of the unit cell. Each of the recognized columns AA and BB as the primary basic structural motifs (BSM_1) is surrounded by eight neighboring columns. The analysis of interaction energies between dimeric BUs belonging to the neighboring columns revealed very close interactions in the directions parallel to the (100) or (001) crystallographic planes and weaker interactions within the diagonal plane (−101) (Table 1). Three types of layers parallel to the (100), (001), or (−101) crystallographic planes may be regarded as possible secondary basic structural motifs (Figure 3). At that, the layers parallel to the (100) crystallographic plane contain columns of only one type (layers AA and layers BB) which are alternated. Within these layers, the dimeric BUs of the neighboring columns are bound mainly by C−H···π interactions. The layers parallel to the (001) plane are mixed and contain columns of both types (layers AB). There are no direction-specific interactions between molecules within these layers. The energy ratios inside and between the layers (100) and (001) are very close (Table 1). It may be explained by the balance of two types of interactions: specific and non-specific. Indeed, the interaction energy between the (100) layers is caused mainly by general dispersion due to the absence of any direction-specific interactions and smaller distance between neighboring planes (7.8 Å). The interaction energy between the (001) layers is caused mainly by C−H···π interactions (the distance between layers is 11.1 Å). As a result, the layer of any type as a secondary basic structural motif (BSM_2) cannot be separated out unambiguously. Therefore, the polymorphic structure **IV** of aspirin may be classified as columnar.

Summarizing the study of pairwise interaction energies in the polymorphic crystals of **I**, **II**, and **IV**, we can conclude that only one plane for the easiest shear deformation may be recognized in structures **I** and **II**, while structure **IV** can be deformed along two crystallographic planes with close probability. However, the question about the direction of the easiest shear deformation along the plane remains open (Figure 5). Polymorphic structure **IV** of aspirin proved to be

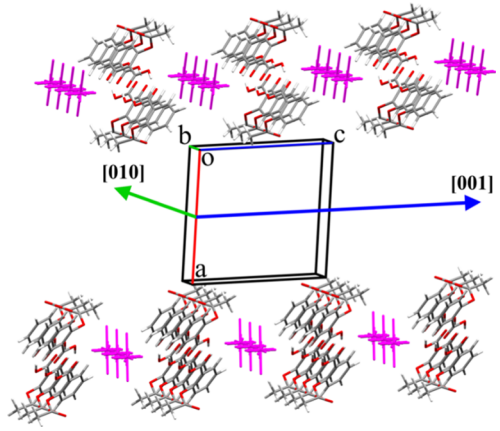

Figure 5. Possible directions of the easiest shear deformation along the (100) crystallographic plane in polymorphic crystals **I** and **II**.

metastable,[49] but the interaction energies between the two visualized types of BSM_2 in structure **IV** are stronger as compared to the interaction energies between BSM_2 in structures **I** and **II** (Table 1). Therefore, it can be presumed that the ability of polymorphic structure **IV** to mechanical response is higher as compared to those in structures **I** and **II** and is caused not only by the interaction energies between the strongly bound fragments of a crystal packing.

https://dx.doi.org/10.1021/acs.cgd.0c01613
Cryst. Growth Des. 2021, 21, 2176−2186

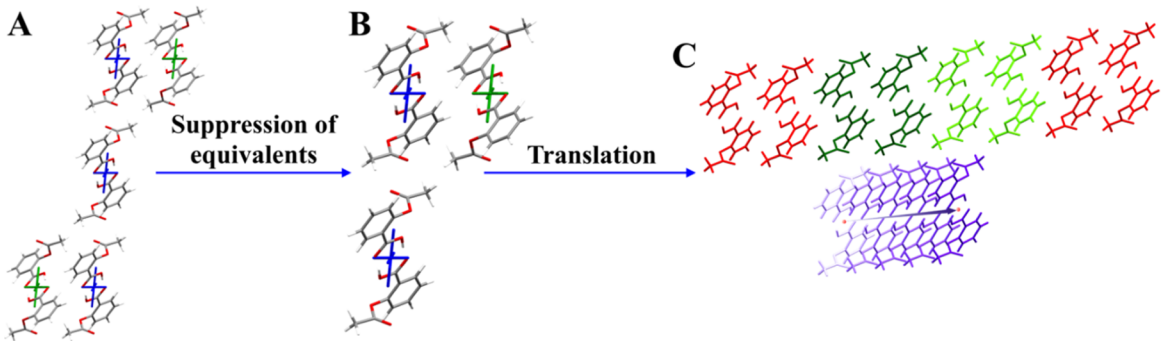

Figure 6. Algorithm of a shear deformation modeling: (a) fragment of a crystal packing containing two layered parts and a BU between them; (b) fragment of one of the symmetry equivalent layers (fixed part) and BU (mobile part) belonging to the neighboring layer; and (c) shift of the BU in relation to the layer fragment.

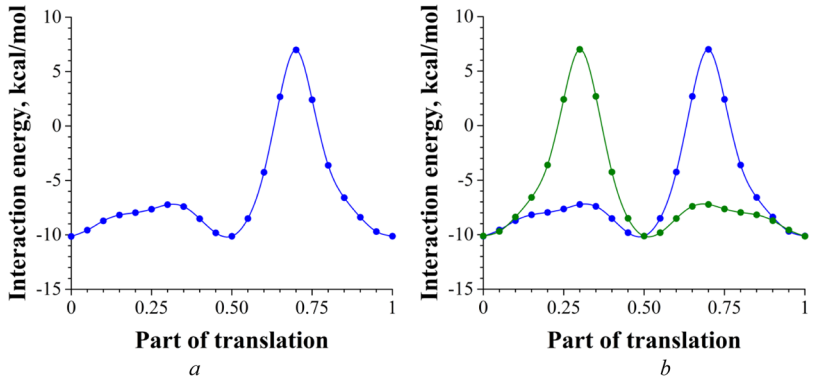

Figure 7. Energy profiles for the mobile part displacement in relation to the fixed part in the [001] direction along the (100) crystallographic plane: the case of direct data order (a) and the overlay of the direct and inverted shift energy profiles (b). Data are shown for polymorphic structure **I**.

Modeling of the Shear Deformation in the Crystal Phase. The attempts to study mechanical properties of organic crystals using mainly periodic calculations or AIMD simulations were performed by different scientific groups.[15−18,20,24,25,39,47,64] To model the crystal structure ability for a shear deformation, we propose the algorithm described in the Experimental Section. To implement such an algorithm, it is necessary to consider the following problems:

1. The minimal size of the rigid unit extracted from the experimental crystal structure and used as a mobile part in the proposed model system.
2. The optimal size of the crystal fragment used as the fixed part, which is necessary to reproduce the shift energy profile in the chosen point group symmetry.
3. The choice of probable crystallographic directions for the displacements.
4. The optimal step size for the displacement.

Each of these problems was considered using well-studied polymorphic structures **I** and **II** of aspirin as model systems.

One BU, defined on the basis of the analysis of pairwise interaction energies and regarded as an elementary structural block of a crystal packing, can be used as a mobile part in the proposed model system. Being bound by symmetry operations, the two neighboring layers are not necessary to complete the information and to delete the equivalents (Figures 6a,b, S4). The size of the fixed part ought to satisfy two conditions at the same time: (a) to be large enough to represent the layer as best as possible; (b) to be small enough so that the calculations of the interaction energies would not be too expensive. Obviously, the fixed part ought to contain all BUs belonging to the first coordination sphere of the mobile part (Figure 6b). This condition ought to be satisfied for the moving BU in all points along the translation trajectory. To do so, the fixed part constructed for the initial geometry should be repeated at least twice in the direction of the mobile part displacement (light green molecules on Figure 6c). Our preliminary modeling of the mobile part translation in the [010] direction within the (100) crystallographic plane has shown the presence of an edge effect. The difference in interaction energies calculated for the BU equivalent positions in relation to the center and edge of the fixed part proved to be up to 0.5 kcal/mol (Figure S6). To avoid edge effect on the calculated energies, the fixed part was expanded by two initial fragments in each direction of the mobile part displacement (red molecules on Figure 6c). The final energy deviations due to the edge effect did not exceed 0.2 kcal/mol (Table S7, Figure S5).

As it was mentioned above, the plane of the easiest deformation of a crystal structure may be recognized using the analysis of pairwise interaction energies. To choose the direction of the shear deformation within the layer, the shortest interatomic distances between the mobile and the fixed parts were estimated along the entire displacement on one crystallographic translation in each of the possible crystallographic directions. If during the translation in a crystallographic direction, an interatomic distance in any point is found to be significantly shorter as compared to the corresponding van der Waals radii sum, this crystallographic direction is excluded from further consideration. Due to the extreme computational cheapness of such calculations, the

https://dx.doi.org/10.1021/acs.cgd.0c01613
Cryst. Growth Des. 2021, 21, 2176−2186

distances were found in each one thousandth of a translation (every 0.024 Å in the case of the longest unit cell parameter).

Since the sliding deformation was modeled as the displacement of the mobile part in relation to the layer fragment as the fixed part, it is necessary to define the step size of such displacement. Being equal to the unit cell parameters, translations in different crystallographic directions within the same structure can have different absolute values (in angstroms). Therefore, it is proposed to define the step size as $1/n$ part of the corresponding translation. In order to evaluate the effect of the step size, energy calculations were performed for a number of geometries where the positions of the mobile part with respect to the fixed part differ by one hundredth of the corresponding translation (Figure S6, Table S8). The error induced by the increasing step size has been defined in comparison to the data obtained within the best approximation. It is only 0.1 kcal/mol in the case of the step size of one twentieth of the corresponding translation length. It should be noted that the step size of one fiftieth caused a slightly higher error value as compared to the step size of one twentieth. Therefore, one-twentieth part of the translation was identified as the most acceptable step size.

Each of the layers is not homogeneous and contains alternating columns of strongly bound dimers with different tilt in relation to the layer mean plane. It means that two types of the BU with different tilt to the neighboring layer can be chosen as a mobile part. To reflect simultaneously the displacement of the BUs of both types in relation to the same layer, the shift energy profiles acquired using all the moments mentioned above should be inverted. In the case of the one-dimensional shift, it is achieved by the reflection of the initial curves in relation to the midpoint of the translation (Figure 7). The energy barrier can be calculated as the difference between maximal and minimal interaction energies of the mobile and fixed parts along the translation path.

Verification of the Proposed Model by the Study of a Shear Deformation in the Aspirin Polymorphic Structures I and II. To verify the proposed model, it was applied for the study of a shear deformation in the well-studied polymorphic structures of aspirin **I** and **II**. The main advantage of these crystals is the availability of many experimental data obtained for them by different methods.[40−42]

The (100) crystallographic plane was found to be the most probable for a shear deformation in aspirin polymorphic structures **I** and **II**. The analysis of minimal distances between molecules of the mobile and fixed part along all the translation trajectory showed that three crystallographic directions for the BU displacement may be considered within this plane (Table 2, Figures S7−S9). At that, the shortest distances between atoms were observed for the displacement in the [001] crystallographic direction. The displacement in the [010] crystallographic direction within the (100) plane was expected to be more preferable due to larger values of minimal distances between atoms (Table 2) in both polymorphic structures under consideration. Such an expectation is also correlated with the data of Burger's vector calculations.[40] Modeling of the dimeric BU displacement in these crystallographic directions allowed us to evaluate the shift energy barriers which proved to be somewhat unexpected. The lowest energy barrier was found for the displacement in the [001] crystallographic direction in polymorphic structures **I** and **II** where the smallest value of the minimal distances was found (Table 2).

Table 2. Minimal Interatomic Distances between Molecules Belonging to the Mobile and Fixed Parts (Å) and Energy Barriers (kcal/mol) for the Displacement of the BU in Different Crystallographic Directions in Polymorphic Crystals I and II of Aspirin

	polymorphic structure **I**		polymorphic structure **II**	
crystallographic direction	minimal distance, Å	energy barrier, kcal/mol	minimal distance, Å	energy barrier, kcal/mol
[010] (100)	1.61	22.1	1.69	20.9
[001] (100)	1.19	17.1	1.26	14.5
[011] (100)	1.46	35.8	1.30	52.4
[100] (001)	1.15	76.1		
[010] (001)	1.41	61.6		
[110] (001)	**0.44**[a]			
[010] (−102)			1.41	58.2
[201] (−102)			1.07	91.2
[211] (−102)			**0.62**	

[a]The values highlighted in bold are too small which makes a shift of the mobile part in that direction impossible.

To explain such an unexpected result, a detailed analysis of relative positions of the BU as a mobile part and molecules belonging to the layer as a fixed fragment along the translation path was performed. It was found that the C−H···O hydrogen bonds were formed during the translation process in both model systems. However, these hydrogen bonds are different. The methyl group of the BU interacts with the carbonyl group of a molecule belonging to the layer fragment (the H···O shortest distance is 1.95 Å) during the displacement in the [010] crystallographic direction (Figure 8a). The displacement of the BU in the [001] crystallographic direction results in formation of the C−H···O hydrogen bonds between the methyl group of a molecule belonging to the layer fragment and the carbonyl group of a molecule belonging to the BU (the H···O shortest distance is 2.36 Å) (Figure 8b). It may be presumed that the formation of stronger hydrogen bonds during the translation along the [010] crystallographic direction results in the higher energy barrier.

Noteworthy is the fact that the systems have positive interaction energies up to 7.0 or 4.4 kcal/mol in some area during the translation of the BU in the [001] crystallographic direction in structures **I** and **II**, respectively, and 11.7 or 10.5 kcal/mol during the translation in the [010] crystallographic direction. Positive interaction energies are caused mainly by strong repulsion between interacted fragments of a crystal packing in unstable positions.

The crystallographic planes (001) and (−102) were identified as alternative BSM_2 in aspirin polymorphic structures **I** and **II** (Table 1). Therefore, these planes may be considered less preferable but possible for the deformation of a crystal packing. Usage of the abovementioned method showed that two crystallographic directions are available for a shear deformation within each of these planes. This was based on the data about minimal distances between atoms (Figures S10, S11). However, energy barriers are very high for the displacement in all these directions (Table 2), so a shear deformation is hardly probable within crystallographic planes (001) in polymorph **I** or (−102) in polymorph **II**.

It should be noted that a thorough study of polymorphs **I** and **II** of aspirin using the nanoindentation method showed that the (100) crystallographic plane and the [010] direction

https://dx.doi.org/10.1021/acs.cgd.0c01613
Cryst. Growth Des. 2021, 21, 2176−2186

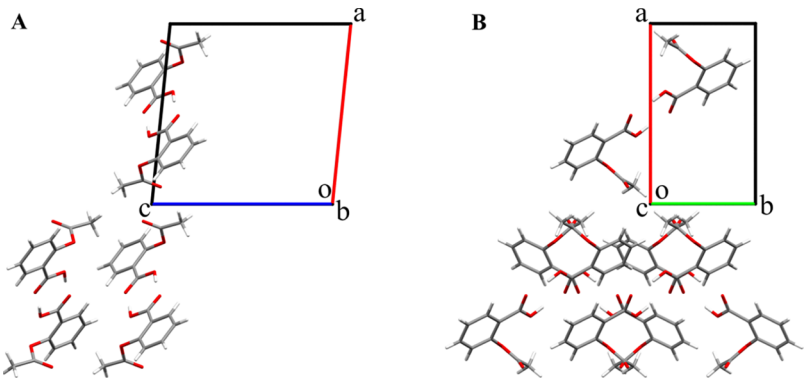

Figure 8. Model system for the study of the dimeric BU displacement in relation to the layer fragment in aspirin polymorphic structures **I** and **II**: (a) in the [010] crystallographic direction and (b) in the [001] crystallographic direction.

within it are the most probable for a shear deformation.[40] Varughese and co-workers[41] confirmed that the (100) is a slip plane, but the most likely direction is [001]. Moreover, the (001) crystallographic plane in polymorph **I** and (−102) plane in polymorph **II** were determined as alternative ones for a shear deformation.[41] Thus, the results of our calculations correlate well with the data obtained by the nanoindentation experimental method. Therefore, the proposed method can be used for prediction of mechanical properties of a crystal structure. Moreover, the data of quantum chemical modeling can solve the dispute about the most probable direction of a shear deformation within the (100) crystallographic plane which is in progress.[48]

Prediction of a Shear Deformation in Polymorphic Structure IV of Aspirin. Polymorphic structure **IV** proved to be metastable,[49] which complicates the study of its properties by experimental methods. The analysis of pairwise interaction energies allowed us to separate out three possible types of BSM_2 (Table 1) among which layers parallel to crystallographic planes (100) and (001) are almost equivalent.

Taking into account the presence of two types of BUs (AA and BB) in this structure, the calculations for a shear deformation modeling were performed for each of them. The analysis of minimal distances between atoms on the translation path showed a high probability for displacement in the [010] direction within each of the three possible crystallographic planes (Tables 3, S9).

Table 3. Minimal Interatomic Distances (Å) and Energy Barriers (kcal/mol) for the Displacement of the BU in Different Crystallographic Directions in Polymorphic Structure IV of Aspirin

	AA basic unit		BB basic unit	
crystallographic direction	minimal distance, Å	energy barrier, kcal/mol	minimal distance, Å	energy barrier, kcal/mol
[010] (100)	1.73	5.4	1.73	5.6
[001] (100)	1.28	22.8	1.28	23.3
[011] (100)	**0.86**		**0.77**	
[100] (001)	**0.37**		**0.37**	
[010] (001)	1.73	9.5	1.73	9.5
[110] (001)	**0.32**		**0.87**	
[010] (−101)	1.82	8.8	1.82	8.4
[101] (−101)	**0.32**		**0.17**	
[111] (−101)	**<0.01**		**0.14**	

The lowest energy barrier (5.4 kcal/mol for AA basic unit or 5.6 kcal/mol for BB basic unit) was calculated for the displacement in the [010] crystallographic direction within the (100) crystallographic plane. The layers containing only one type of the BUs were found to be parallel to this plane. The BU displacement along the (001) crystallographic plane should overcome the energy barrier which is almost twice as high (9.5 kcal/mol) compared to the lowest energy barrier. A detailed study of two model systems (Figure 9) revealed that non-directed interactions like hydrogen bonds are formed during the displacement within the (100) crystallographic plane. The displacement of the BU within the (001) crystallographic plane results in formation of a very weak C_{ar}–H···O hydrogen bond (the shortest H···O distance is 2.43 Å). It can be presumed that formation of directional interaction results in increasing of the shift energy barrier.

The displacement in the [010] crystallographic direction within the diagonal (−101) crystallographic plane (Figure S12) has the energy barrier which is very close to the one within the (001) crystallographic plane. All the calculated energy barriers in polymorphic structure **IV** are lower than the smallest energy barrier in structures **I** and **II**. Moreover, the highest interaction energy between the mobile and the fixed parts during displacements in the [010] direction within any of the three crystallographic planes is not positive, contrary to those found in structures **I** and **II**. This means the absence of any steric repulsion during the displacement of the AA or BB columns (separated out as BSM_1) in the [010] crystallographic direction. These data confirm our classification of aspirin polymorphic structure **IV** as columnar and may explain the low stability of this crystal form.

CONCLUSIONS

A new method is proposed for the study of mechanical properties of molecular crystals using quantum chemical modeling. This method consists of two steps. In the first stage, a study of the pairwise interaction energies was performed. Based on calculated interaction energies, strongly bound fragments of a crystal packing were separated out as well as the planes for the easiest shear deformation. In the second stage, one BU from the BSM_2 as a mobile part and the fragment of the neighboring BSM_2 as a fixed part were used for the simulation of shear deformation. The initial geometries of all fragments of this model system were extracted from the crystal experimental data. The analysis of minimal distances between atoms of the mobile and fixed parts gives opportunity

https://dx.doi.org/10.1021/acs.cgd.0c01613
Cryst. Growth Des. 2021, 21, 2176−2186

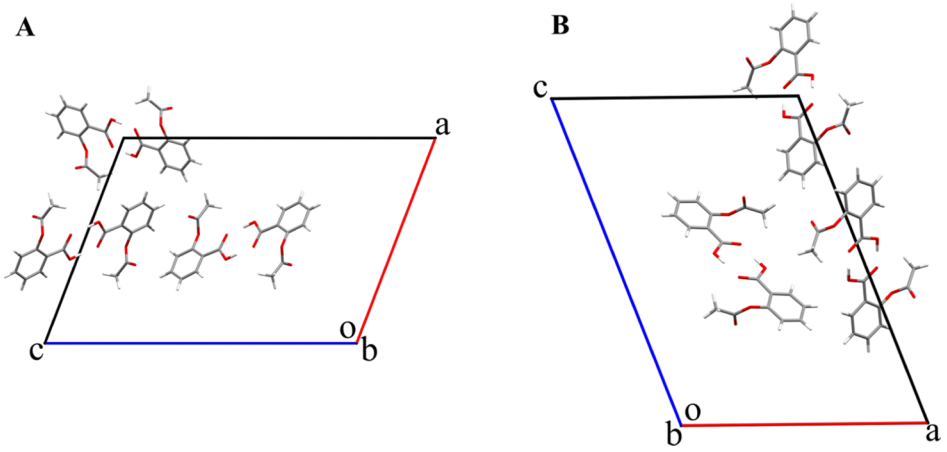

Figure 9. Model system for the study of the dimeric BU displacement in the [010] direction in aspirin polymorphic structure **IV**: (a) within the (100) crystallographic plane and (b) within the (001) crystallographic plane.

to define possible directions of the BU displacement with respect to the layer. The mobile part was displaced with a certain step size on one crystallographic translation, and the interaction energies between it and the fixed part have been calculated. The shift energy profile was constructed as a set of interaction energies calculated at each of the points along the translation. The energy barrier for the displacement of the mobile part with respect to the fixed part was calculated as a difference between the highest and the lowest interaction energies on the displacement path.

The proposed algorithm was tested on the well-studied polymorphic structures **I** and **II** of aspirin. It was revealed that the [001] crystallographic direction within the (100) crystallographic plane is the most likely for a shear deformation. The deformation in the [010] direction within the same plane needs more energy due to the necessity to break C−H···O hydrogen bonds formed between the mobile and fixed parts during the translation. The results of our study correlate well with the experimental data obtained by the nanoindentation method for polymorphic structures **I** and **II**. Therefore, this approach can be used to predict the mechanical properties of a little studied structure. The corresponding analysis was carried out for the newest aspirin polymorphic structure **IV**, which is metastable and cannot be studied by experimental methods. It was revealed that this structure is columnar. The most probable direction of a shear deformation is the [010] crystallographic direction within the (100) crystallographic plane according to the smallest calculated energy barrier as compared to similar values for the displacements in other possible directions. The highest interaction energy during the displacement in the [010] crystallographic direction proved to be negative, which may explain the ability of polymorphic structure **IV** to be destroyed easily.

■ ASSOCIATED CONTENT

Supporting Information

The Supporting Information is available free of charge at https://pubs.acs.org/doi/10.1021/acs.cgd.0c01613.

> Pairwise interaction energies between molecules, interaction energy differences arising due to the edge effect and different step sizes, crystal packing along different crystallographic directions in terms of molecules and EVDs, profiles of interaction energies, and minimal interatomic distances for the translation in different directions (PDF)

■ AUTHOR INFORMATION

Corresponding Author

Svitlana V. Shishkina − *V.N. Karazin Kharkiv National University, Kharkiv 61022, Ukraine; SSI "Institute for Single Crystals" NAS of Ukraine, Kharkiv 61001, Ukraine;* orcid.org/0000-0002-3946-1061; Phone: +38 066 771 87 42; Email: sveta@xray.isc.kharkov.com

Authors

Yevhenii Vaksler − *Laboratoire de Spectroscopie pour les Interactions, la Réactivité et l'environnement (UMR CNRS A8516), Université de Lille, 59655 Villeneuve d'Ascq Cedex, France; V.N. Karazin Kharkiv National University, Kharkiv 61022, Ukraine; SSI "Institute for Single Crystals" NAS of Ukraine, Kharkiv 61001, Ukraine*

Abdenacer Idrissi − *Laboratoire de Spectroscopie pour les Interactions, la Réactivité et l'environnement (UMR CNRS A8516), Université de Lille, 59655 Villeneuve d'Ascq Cedex, France*

Victoriya V. Urzhuntseva − *V.N. Karazin Kharkiv National University, Kharkiv 61022, Ukraine*

Complete contact information is available at: https://pubs.acs.org/10.1021/acs.cgd.0c01613

Author Contributions

Y.V. performed quantum chemical calculations, analyzed the results, and wrote the manuscript; A.I. discussed the results; V.U. contributed to the crystal structure analysis; and S.S. generated the idea, analyzed the results, and wrote the manuscript.

Notes

The authors declare no competing financial interest.

■ REFERENCES

(1) Lee, A. Y.; Erdemir, D.; Myerson, A. S. Crystal polymorphism in chemical process development. *Annu. Rev. Chem. Biomol. Eng.* **2011**, *2*, 259−280.

(2) Bernstein, J. *Polymorphism in Molecular Crystals*; Oxford University Press Inc.: New York, 2002.

(3) Miller, S. P. F.; Raw, A. S.; Yu, L. X. Scientific considerations of pharmaceutical solid polymorphism in regulatory applications. In

Polymorphism in the Pharmaceutical Industry; Hilfiker, R.; Wiley-VCH: Weinheim, 2006; pp. 385−405.
(4) Fabbiani, F. P. A.; Allan, D. R.; David, W. I. F.; Davidson, A. J.; Lennie, A. R.; Parsons, S.; Pulham, C. R.; Warren, J. E. High-Pressure Studies of Pharmaceuticals: An Exploration of the Behavior of Piracetam. *Cryst. Growth Des.* **2007**, *7*, 1115−1124.
(5) Seryotkin, Y. V.; Drebushchak, T. N.; Boldyreva, E. V. A high-pressure polymorph of chlorpropamide formed on hydrostatic compression of the α-form in saturated ethanol solution. *Acta Crystallogr., Sect. B: Struct. Sci., Cryst. Eng. Mater.* **2013**, *69*, 77−85.
(6) Zieliński, W.; Katrusiak, A. Hydrate smaller than the anhydrate. *CrystEngComm* **2015**, *17*, 5468−5473.
(7) Moggach, S. A.; Lennie, A. R.; Morrison, C. A.; Richardson, P.; Stefanowicz, F. A.; Warren, J. E. Pressure induced phase transitions in the tripeptide glutathione to 5.24 GPa: the crystal structure of glutathione-II at 2.94 GPa and glutathione-III at 3.70 GPa. *CrystEngComm* **2010**, *12*, 2587−2595.
(8) Boldyreva, E. V.; Ivashevskaya, S. N.; Sowa, H.; Ahsbahs, H.; Weber, H.-P. Effect of hydrostatic pressure on the γ-polymorph of glycine. 1. A polymorphic transition into a new δ-form. *Z. Kristallogr.-Cryst. Mater.* **2005**, *220*, 50−57.
(9) Oswald, I. D. H.; Lennie, A. R.; Pulham, C. R.; Shankland, K. High-pressure structural studies of the pharmaceutical, chlorothiazide. *CrystEngComm* **2010**, *12*, 2533−2540.
(10) Johnstone, R. D. L.; Lennie, A. R.; Parker, S. F.; Parsons, S.; Pidcock, E.; Richardson, P. R.; Warren, J. E.; Wood, P. A. High-pressure polymorphism in salicylamide. *CrystEngComm* **2010**, *12*, 1065−1078.
(11) Chemburkar, S. R.; Bauer, J.; Deming, K.; Spiwek, H.; Patel, K.; Morris, J.; Henry, R.; Spanton, S.; Dziki, W.; Porter, W.; Quick, J.; Bauer, P.; Donaubauer, J.; Narayanan, B. A.; Soldani, M.; Riley, D.; McFarland, K. Dealing with the impact of ritonavir polymorphs on the late stages of bulk drug process development. *Org. Process Res. Dev.* **2000**, *4*, 413−417.
(12) Armstrong, R. W.; Walley, S. M.; Elban, W. L. Crystal indentation hardness. In *Crystal Indentation Hardness*; Armstrong, R. W.; Walley, S. M.; Elban, W. L., Eds.; MDPI AG: Basel, 2018; pp 1−9.
(13) *High-Pressure Crystallography*; Katrusiak, A., McMillan, P., Eds.; Springer Science & Business Media, LCC: New York, 2004.
(14) *High-Pressure Crystallography. From Fundamental Phenomena to Technological Applications*; Boldyreva, E.; Dera, P., Eds.; Springer Science & Business Media, LCC: Dordrecht, 2010.
(15) Wang, C.; Sun, C. C. Computational techniques for predicting mechanical properties of organic crystals: a systematic evaluation. *Mol. Pharmaceutics* **2019**, *16*, 1732−1741.
(16) Sun, C. C.; Kiang, Y.-H. On the identification of slip planes in organic crystals based on attachment energy calculation. *J. Pharm. Sci.* **2008**, *97*, 3456−3461.
(17) Golesorkhtabar, R.; Pavone, P.; Spitaler, J.; Puschnig, P.; Draxl, C. Elastic: a tool for calculating second-order elastic constants from first principles. *Comput. Phys. Commun.* **2013**, *184*, 1861−1873.
(18) Day, G. M.; Price, S. L.; Leslie, M. Elastic constant calculations for molecular organic crystals. *Cryst. Growth Des.* **2001**, *1*, 13−27.
(19) Shishkin, O. V.; Zubatyuk, R. I.; Shishkina, S. V.; Dyakonenko, V. V.; Medviediev, V. V. Role of supramolecular synthons in the formation of the supramolecular architecture of molecular crystals revisited from an energetic viewpoint. *Phys. Chem. Chem. Phys.* **2014**, *16*, 6773−6786.
(20) Turner, M. J.; Thomas, S. P.; Shi, M. W.; Jayatilaka, D.; Spackman, M. A. Energy frameworks: insights into interaction anisotropy and the mechanical properties of molecular crystals. *Chem. Commun.* **2015**, *51*, 3735−3738.
(21) Shishkina, S. V. Using of quantum-chemical calculations to molecular crystals studying. *Struct. Chem.* **2019**, *30*, 1565−1577.
(22) Reddy, C. M.; Gundakaram, R. C.; Basavoju, S.; Kirchner, M. T.; Padmanabhan, K. A.; Desiraju, G. R. Structural basis for bending of organic crystals. *Chem. Commun.* **2005**, *41*, 3945−3947.
(23) Thomas, S. P.; Shi, M. W.; Koutsantonis, G. A.; Jayatilaka, D.; Edwards, A. J.; Spackman, M. A. The elusive structural origin of plastic bending in dimethyl sulfone crystals with quasi-isotropic crystal packing. *Angew. Chem., Int. Ed.* **2017**, *129*, 8588−8592.
(24) Wang, C.; Sun, C. C. Identifying slip planes in organic polymorphs by combined energy framework calculations and topology analysis. *Cryst. Growth Des.* **2018**, *18*, 1909−1916.
(25) Bal Raju, K.; Ranjan, S.; Vishnu, V. S.; Bhattacharya, M.; Bhattacharya, B.; Mukhopadhyay, A. K.; Malla Reddy, C. Rationalizing distinct mechanical properties of three polymorphs of a drug adduct by nanoindentation and energy frameworks analysis: role of slip layer topology and weak interactions. *Cryst. Growth Des.* **2018**, *18*, 3927−3937.
(26) Mishra, M. K.; Sun, C. C. Conformation directed interaction anisotropy leading to distinct bending behaviors of two Roy polymorphs. *Cryst. Growth Des.* **2020**, *20*, 4764−4769.
(27) Ghosh, S.; Mondal, A.; Kiran, M. S. R. N.; Ramamurty, U.; Reddy, C. M. The role of weak interactions in the phase transition and distinct mechanical behavior of two structurally similar caffeine co-crystal polymorphs studied by nanoindentation. *Cryst. Growth Des.* **2013**, *13*, 4435−4441.
(28) Bu, R.; Xie, W.; Zhang, C. Heat-induced polymorphic transformation facilitating the low impact-sensitivity of 2,2-dinitroethylene-1,1-diamine (FOX-7). *J. Phys. Chem. C* **2019**, *123*, 16014−16022.
(29) Tawashi, R. Aspirin: dissolution rates of two polymorphic forms. *Science* **1968**, *160*, 76.
(30) Mulley, B. A.; Rye, R. M.; Shaw, P. Further evidence on the question of polymorphism in aspirin. *J. Pharm. Pharmacol.* **1971**, *23*, 902−904.
(31) Schwartzman, G. Does aspirin exist in polymorphic states? *J. Pharm. Pharmacol.* **1972**, *24*, 169−170.
(32) Kildsig, D. O.; Denbo, R.; Peck, G. E. Structural differences in solutions derived from polymorphic modifications of aspirin. *J. Pharm. Pharmacol.* **1971**, *23*, 374−376.
(33) Mitchell, A. G.; Milaire, B. L.; Saville, D. J.; Griffiths, R. V. Aspirin dissolution: polymorphism, crystal habit or crystal defects. *J. Pharm. Pharmacol.* **1971**, *23*, 534−535.
(34) Watanabe, A.; Yamaoka, Y.; Takada, K. Crystal habits and dissolution behavior of aspirin. *Chem. Pharm. Bull.* **1982**, *30*, 2958−2963.
(35) Vishweshwar, P.; McMahon, J. A.; Oliveira, M.; Peterson, M. L.; Zaworotko, M. J. The predictably elusive form II of aspirin. *J. Am. Chem. Soc.* **2005**, *127*, 16802−16803.
(36) Bond, A. D.; Boese, R.; Desiraju, G. R. On the polymorphism of aspirin. *Angew. Chem., Int. Ed.* **2007**, *46*, 615−617.
(37) Bond, A. D.; Boese, R.; Desiraju, G. R. On the polymorphism of aspirin: crystalline aspirin as intergrowths of two "polymorphic" domains. *Angew. Chem., Int. Ed.* **2007**, *46*, 618−622.
(38) Bond, A. D.; Solanko, K. A.; Parsons, S.; Redder, S.; Boese, R. Single crystals of aspirin form II: crystallisation and stability. *CrystEngComm* **2011**, *13*, 399−401.
(39) Bauer, J. D.; Haussühl, E.; Winkler, B.; Arbeck, D.; Milman, V.; Robertson, S. Elastic properties, thermal expansion, and polymorphism of acetylsalicylic acid. *Cryst. Growth Des.* **2010**, *10*, 3132−3140.
(40) Olusanmi, D.; Roberts, K. J.; Ghadiri, M.; Ding, Y. The breakage behaviour of aspirin under quasi-static indentation and single particle impact loading: effect of crystallographic anisotropy. *Int. J. Pharm.* **2011**, *411*, 49−63.
(41) Varughese, S.; Kiran, M. S. R. N.; Solanko, K. A.; Bond, A. D.; Ramamurty, U.; Desiraju, G. R. Interaction anisotropy and shear instability of aspirin polymorphs established by nanoindentation. *Chem. Sci.* **2011**, *2*, 2236−2242.
(42) Crowell, E. L.; Dreger, Z. A.; Gupta, Y. M. High-pressure polymorphism of acetylsalicylic acid (aspirin): Raman spectroscopy. *J. Mol. Struct.* **2015**, *1082*, 29−37.

https://dx.doi.org/10.1021/acs.cgd.0c01613
Cryst. Growth Des. 2021, 21, 2176−2186

(43) Mittal, A.; Malhotra, D.; Jain, P.; Kalia, A.; Shunmugaperumal, T. Studies on aspirin crystals generated by a modified vapor diffusion method. *AAPS PharmSciTech* **2016**, *17*, 988−994.
(44) Wen, S.; Beran, G. J. O. Accidental degeneracy in crystalline aspirin: new insights from high-level ab initio calculations. *Cryst. Growth Des.* **2012**, *12*, 2169−2172.
(45) Reilly, A. M.; Tkatchenko, A. Role of dispersion interactions in the polymorphism and entropic stabilization of the aspirin crystal. *Phys. Rev. Lett.* **2014**, *113*, 055701.
(46) Adhikari, K.; Flurchick, K. M.; Valenzano, L. A hybrid density functional study on the effects of pressure on paracetamol and aspirin polymorphs. *Comput. Theor. Chem.* **2015**, *1062*, 90−98.
(47) LeBlanc, L. M.; Otero-de-la-Roza, A.; Johnson, E. R. Evaluation of shear-slip transitions in crystalline aspirin by density-functional theory. *Cryst. Growth Des.* **2016**, *16*, 6867−6873.
(48) Gabriele, B. P. A.; Williams, C. J.; Lauer, M. E.; Derby, B.; Cruz-Cabeza, A. J. Nanoindentation of molecular crystals: lessonf learned from aspirin. *Cryst. Growth Des.* **2020**, *20*, 5956−5966.
(49) Shtukenberg, A. G.; Hu, C. T.; Zhu, Q.; Schmidt, M. U.; Xu, W.; Tan, M.; Kahr, B. The third ambient aspirin polymorph. *Cryst. Growth Des.* **2017**, *17*, 3562−3566.
(50) Groom, C. R.; Bruno, I. J.; Lightfoot, M. P.; Ward, S. C. The Cambridge Structural Database. *Acta Crystallogr., Sect. B: Struct. Sci., Cryst. Eng. Mater.* **2016**, *72*, 171−179.
(51) Konovalova, I. S.; Shishkina, S. V.; Paponov, B. V.; Shishkin, O. V. Analysis of the crystal structure of two polymorphic modifications of 3,4-diamino-1,2,4-triazole based on the energy of the intermolecular interactions. *CrystEngComm* **2010**, *12*, 909−916.
(52) Shishkin, O. V.; Dyakonenko, V. V.; Maleev, A. V. Supramolecular architecture of crystals of fused hydrocarbons based on topology of intermolecular interactions. *CrystEngComm* **2012**, *14*, 1795−1804.
(53) Macrae, C. F.; Bruno, I. J.; Chisholm, J. A.; Edgington, P. R.; McCabe, P.; Pidcock, E.; Rodriguez-Monge, L.; Taylor, R.; van de Streek, J.; Wood, P. A. Mercury CSD 2.0- new features for the visualization and investigation of crystal structures. *J. Appl. Crystallogr.* **2008**, *41*, 466−470.
(54) Coppens, P. The use of a polarized hydrogen atom in X-ray structure refinement. *Acta Crystallogr., Sect. B: Struct. Crystallogr. Cryst. Chem.* **1972**, *28*, 1638−1640.
(55) Allen, F. H.; Bruno, I. J. Bond lengths in organic and metal-organic compounds revisited: X-H bond lengths from neutron diffraction data. *Acta Crystallogr., Sect. B: Struct. Sci.* **2010**, *66*, 380−386.
(56) Grimme, S.; Ehrlich, S.; Goerigk, L. Effect of the damping function in dispersion corrected density functional theory. *J. Comput. Chem.* **2011**, *32*, 1456−1465.
(57) Weigend, F.; Ahlrichs, R. Balanced basis sets of split valence, triple zeta valence and quadruple zeta valence quality for H to Rn: design and assessment of accuracy. *Phys. Chem. Chem. Phys.* **2005**, *7*, 3297−3305.
(58) Weigend, F. Accurate Coulomb-fitting basis sets for H to Rn. *Phys. Chem. Chem. Phys.* **2006**, *8*, 1057−1065.
(59) Boys, S. F.; Bernardi, F. The calculation of small molecular interactions by the differences of separate total energies. Some procedures with reduced errors. *Mol. Phys.* **1970**, *19*, 553−566.
(60) Shishkin, O. V.; Zubatyuk, R. I.; Maleev, A. V.; Boese, R. Investigation of topology of intermolecular interactions in the benzene-acetylene co-crystal by different theoretical methods. *Struct. Chem.* **2014**, *25*, 1547−1552.
(61) Frisch, M. J.; Trucks, G. W.; Schlegel, H. B.; Scuseria, G. E.; Robb, M. A.; Cheeseman, J. R.; Montgomery, J. A., Jr.; Vreven, T.; Kudin, K. N.; Burant, J. C.; Millam, J. M.; Iyengar, S. S.; Tomasi, J.; Barone, V.; Mennucci, B.; Cossi, M.; Scalmani, G.; Rega, N.; Petersson, G. A.; Nakatsuji, H.; Hada, M.; Ehara, M.; Toyota, K.; Fukuda, R.; Hasegawa, J.; Ishida, M.; Nakajima, T.; Honda, Y.; Kitao, O.; Nakai, H.; Klene, M.; Li, X.; Knox, J. E.; Hratchian, H. P.; Cross, J. B.; Bakken, V.; Adamo, C.; Jaramillo, J.; Gomperts, R.; Stratmann, R. E.; Yazyev, O.; Austin, A. J.; Cammi, R.; Pomelli, C.; Ochterski, J. W.; Ayala, P. Y.; Morokuma, K.; Voth, G. A.; Salvador, P.; Dannenberg, J. J.; Zakrzewski, V. G.; Dapprich, S.; Daniels, A. D.; Strain, M. C.; Farkas, O.; Malick, D. K.; Rabuck, A. D.; Raghavachari, K.; Foresman, J. B.; Ortiz, J. V.; Cui, Q.; Baboul, A. G.; Clifford, S.; Cioslowski, J.; Stefanov, B. B.; Liu, G.; Liashenko, A.; Piskorz, P.; Komaromi, I.; Martin, R. L.; Fox, D. J.; Keith, T.; Al-Laham, M. A.; Peng, C. Y.; Nanayakkara, A.; Challacombe, M.; Gill, P. M. W.; Johnson, B.; Chen, W.; Wong, M. W.; Gonzalez, C.; Pople, J. A. *Gaussian 03*, Revision C.02; Gaussian, Inc.: Wallingford CT, 2004.
(62) Dunning, T. H., Jr. Gaussian basis sets for use in correlated molecular calculations. I. The atoms boron through neon and hydrogen. *J. Chem. Phys.* **1989**, *90*, 1007−1023.
(63) Davidson, E. R. Comment on "Comment on Dunning's correlation-consistent basis sets". *Chem. Phys. Lett.* **1996**, *260*, 514−518.
(64) Li, Q.; Bond, A. D.; Zeitler, J. A. Studying mechanical properties and phase transition of aspirin polymorphs with terahertz spectroscopy and ab initio simulations. *2019 44th International Conference on Infrared, Millimeter, and Terahertz Waves (IRMMW-THz)*, 2019, Paris, France, pp 1−2.

https://dx.doi.org/10.1021/acs.cgd.0c01613
Cryst. Growth Des. 2021, 21, 2176−2186